



Pressure-induced polyamorphism in lanthanide-solute metallic glasses

Liangliang Li^{1,2}, Luhong Wang^{*1}, Renfeng Li^{1,2}, Dongdong Qu³, Haiyan Zhao^{4,5}, Karena W. Chapman⁴, Peter J. Chupas⁴, and Haozhe Liu^{**1,2}

HPSTAR
480-2017

¹ Harbin Institute of Technology, Harbin 150080, P.R. China

² Center for High Pressure Science Technology Advanced Research, Changchun 130015, P.R. China

³ School of Mechanical and Mining Engineering, The University of Queensland, Brisbane, Queensland 4072, Australia

⁴ X-ray Science Division, Advanced Photon Source, Argonne National Laboratory, Argonne, Illinois 60439, USA

⁵ Center for Advanced Energy Studies, University of Idaho, Idaho Falls, Idaho 83406, USA

Received 20 March 2017, revised 10 April 2017, accepted 18 April 2017

Published online 27 April 2017

Keywords high pressure, metallic glasses, pair distribution function, polyamorphism

* Corresponding author: e-mail luhong1@hit.edu.cn, Phone/Fax: +86451 86403249

** e-mail haozhe.liu@hpstar.ac.cn, Phone: +8610 56981748

The electronic structure inheritance of lanthanide-solute atoms in lanthanide-based metallic glasses has been proposed. Is a polyamorphism possible in lanthanide-solute metallic glasses? So far, polyamorphic phase transitions in metallic glass containing lanthanide have been observed only in lanthanide-solute metallic glasses. Here, a pressure-induced transition between two distinct amorphous states, accompanied by a 7% volume collapse at ambient pressure, was observed in $\text{La}_{43.4}\text{Pr}_{18.6}\text{Al}_{14}\text{Cu}_{24}$ metallic glass, with low lanthanide

content, by using *in situ* X-ray total scattering method. The transformation also indicated by changes in short range and medium range order. Thus, it is proposed that the lanthanide-solute metallic glasses also inherit *4f* electronic transition from pure lanthanide element in polyamorphic transition. This discovery offers a supplement to research on lanthanide-based metallic glasses, which further provides a new perspective of the polyamorphic transformation in metallic glasses containing lanthanide element.

© 2017 WILEY-VCH Verlag GmbH & Co. KGaA, Weinheim

1 Introduction Pressure-induced polyamorphism in traditional network-forming glassy state materials has been reported, such as, in ice, silica, and silicon [1–4]. Generally, this polyamorphism tends to involve an open packed structure transforming to a more densely packed one, namely, an increase in atomic coordination under pressure [4, 5]. Metallic glasses, as a new member of the glass family, are distinct from the traditional network-forming glasses since they have non-directional metallic bonds in nature [6, 7]. The new member also exhibits polyamorphism induced by pressure [7–10], although they are spatially densely-packed and they have the maximum coordination number already [11]. The polyamorphism transformation from low density amorphous state (LDAS) to high density amorphous state (HDAS) induced by pressure was found firstly in Ce-based metallic glasses, such as $\text{Ce}_{55}\text{Al}_{45}$, $\text{Ce}_{75}\text{Al}_{25}$, $\text{Ce}_{75}\text{Al}_{23}\text{Si}_2$, and $\text{Ce}_{65}\text{Co}_{25}\text{Al}_{10}$ [7–10]. The transition mechanism was ascribed to *4f* electron delocalization in Ce under high pressure in experiment and

theory [7, 8]. Generally, this polyamorphic phase transformation is viewed as first-order transition. At ambient conditions, the electronic configuration of the lanthanides is characterized by $4f^n(5d6s)^3$, where *n* varies from 0 to 14 corresponding to lanthanum to lutetium [12]. Thus, the polyamorphism transformation induced by pressure was expected in other lanthanide-based metallic glasses, in which lanthanum should be excluded due to the absence of *4f* electron. Indeed, the lanthanum-based metallic glass does not display a polyamorphic transition upon compression [13], whereas, the polyamorphism transition caused by *4f* electronic delocalization has been also reported in other rare earth element-based metallic glasses subsequently, such as $\text{Gd}_{40}\text{Y}_{16}\text{Al}_{24}\text{Co}_{20}$ and $\text{Pr}_{60}\text{Cu}_{20}\text{Al}_{10}\text{Ni}_{10}$ [14]. These polyamorphism transformations demonstrate the electronic structure inheritance of lanthanide-solute atoms in lanthanide-based metallic glasses [14]. All of these polyamorphism transitions were found in metallic glasses with high lanthanide content. Thus, it raises an interesting

question: does this polyamorphism transformation occur in lanthanide-solute metallic glasses? In other words, does this inheritance exist in metallic glasses with low lanthanide content? To shed light on this problem, metallic glass with low lanthanide content was studied under compressed conditions by means of synchrotron X-ray total scattering method, focusing on a member of this family, namely $\text{La}_{43.4}\text{Pr}_{18.6}\text{Al}_{14}\text{Cu}_{24}$ metallic glass.

2 Experimental The $\text{La}_{43.4}\text{Pr}_{18.6}\text{Al}_{14}\text{Cu}_{24}$ metallic glass ribbon was prepared by melt spinning. First, an ingot with the nominal composition $\text{La}_{43.4}\text{Pr}_{18.6}\text{Al}_{14}\text{Cu}_{24}$ was prepared by arc melting the high purity (over 99.9 wt.%) elements La, Pr, Al, and Cu protected by highly purified argon gas. To assure the homogeneity of the elements, the ingot was remelted for at least three times. After that, the prepared ingot was put into a quartz tube and melted by induction heating under high vacuum condition ($\sim 6.6 \times 10^{-3}$ Pa). Then, glassy ribbons with a thickness of $25 \mu\text{m}$ were obtained by rapidly quenching the molten alloy onto a fast spinning copper wheel.

Total synchrotron X-ray scattering data of the $\text{La}_{43.4}\text{Pr}_{18.6}\text{Al}_{14}\text{Cu}_{24}$ metallic glass were collected at the sector 11-ID-B beamline at the Advanced Photon Source, Argonne National Laboratory with the incident beam size $150 \times 150 \mu\text{m}^2$ and an 86.7 keV high energy. A 2D large amorphous-silicon-based flat-panel detector with 2048×2048 pixels (unbinned) covering a 41×41 cm active area was used to record the synchrotron X-ray scattering patterns. Images consisting of a summation of 150 5 s exposures provided an adequate signal-to-noise ratio at each pressure. The sample with width of $130 \mu\text{m}$, length of $140 \mu\text{m}$, and thickness of $25 \mu\text{m}$ was located in the sample chamber, which is T301 stainless steel gasket with $270 \mu\text{m}$ diameter hole between two diamond anvils with culet size of $500 \mu\text{m}$. 1:4 methanol/ethanol and ruby were used as pressure medium and marker, respectively. The pressure was up to 40.5 GPa and measured by the ruby fluorescence method.

Raw image data were processed using software Fit-2D [15]. After removing the diamond peaks with masking strategy [16], one-dimensional scattering data were obtained. Subtracting the contributions from the sample environment and background, which was measured through pure pressure medium loaded in gasket hole between anvils, the reduced pair distribution function (PDF) $G(r)$ and structure factor $S(Q)$ were extracted using the program PDFgetX2 [17], which performed a numerical Fourier transform of $S(Q)$ according to

$$G(r) = \frac{2}{\pi} \int_0^{\infty} Q[S(Q) - 1] \sin(Qr) dQ. \quad (1)$$

Compton scattering from the sample was corrected based on tabulated values for the known sample composition. The detector response was corrected using established geometric corrections with transmission coefficient for the

0.5 mm detector phosphor of 0.8 at ~ 86.7 keV. The first peaks position of both $S(Q)$ and $G(r)$ were estimated from the peak fitting using a pseudo-Voigt profile function.

3 Results and discussion Figure 1 displays the structure factor $S(Q)$ and corresponding PDFs of the $\text{La}_{43.4}\text{Pr}_{18.6}\text{Al}_{14}\text{Cu}_{24}$ metallic glass derived from synchrotron X-ray scattering experiment as a function of pressure. Absence of sharp peaks in $S(Q)$ and PDFs suggests that the sample remains fully amorphous state within the applied pressure range. As expected for the densification effect of pressure, first peak position Q_1 of structure factor $S(Q)$ in reciprocal space shifts toward higher momentum transfer and the nearest-neighbor distance r_1 in real space moves to shorter distance with increasing pressure. As pressure increases, in real space the left-hand shoulder on first peak gradually disappearing and the right-hand shoulder of second peak increasingly developing indicate the structural changes in short and medium range order, respectively. The splitting of the second peak in both $S(Q)$ and PDFs observed at applied pressure is the characteristic indicator for

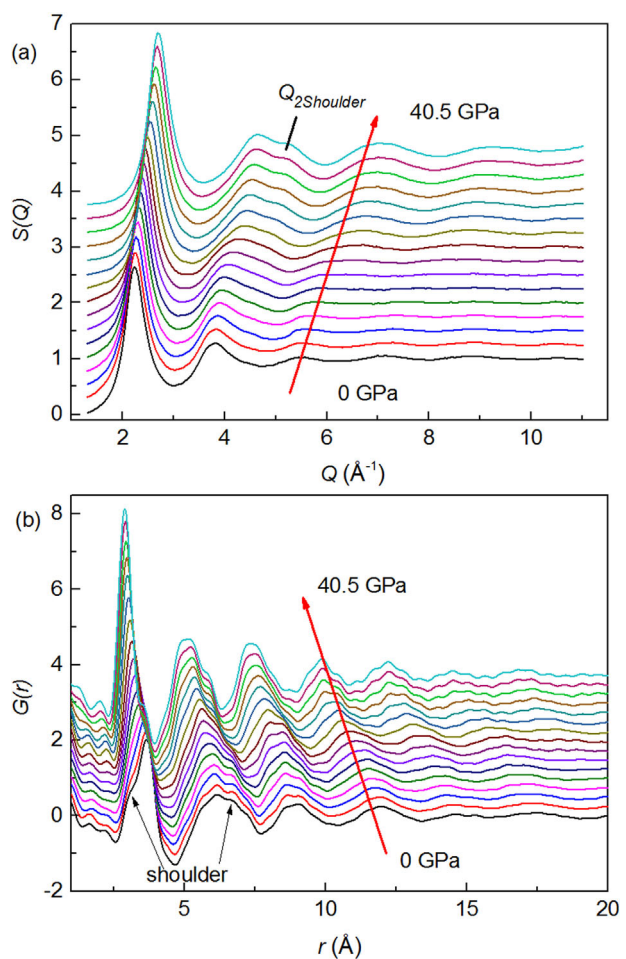


Figure 1 (a) Structure factor $S(Q)$ and (b) pair distribution function $G(r)$ of the $\text{La}_{43.4}\text{Pr}_{18.6}\text{Al}_{14}\text{Cu}_{24}$ metallic glass at various pressure conditions.

conventional amorphous alloy systems [18, 19]. As generally accepted, the Q_1 mainly reflects the medium range order correlation in real space, while the high- Q peaks embody more short range order features. In reciprocal space, a shoulder developing on the second peak signifies the occurrence of pressure-induced structural changes in short range order. Moreover, the structure changes can be further illustrated by the differential structure factor $S(Q)$ and PDFs which are calculated by subtracting the structure factor $S(Q)$ and PDFs at 0 GPa from higher pressure data, respectively. This indicates the sequence of changes in the structure, as shown in Fig. 2. These differential structure factors $S(Q)$ under pressure present the discontinuous change of slope of the first peak and nadir, and display a developing shoulder on the second peak. Whereas for differential PDFs, both the first peak and nadir show a discontinuous slope change and second peak exhibits an interchange of status between peak and shoulder, as pressure increases. All these observed structural changes in the short and medium range length scale should reflect in the relations of both $P-Q_1$ and $P-r_1$, by which the exact transition region can be determined.

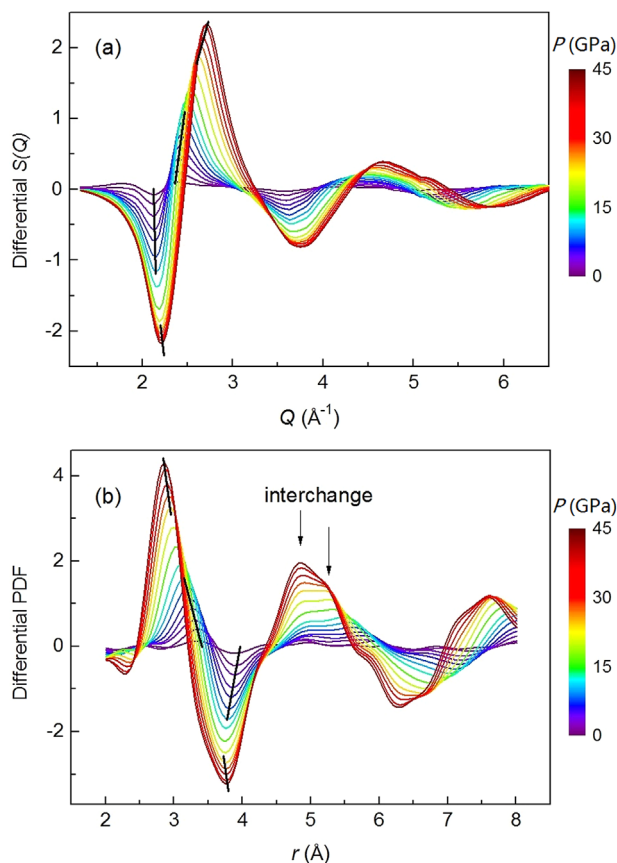


Figure 2 (a) Differential structure factor and (b) differential PDFs of the $\text{La}_{43.4}\text{Pr}_{18.6}\text{Al}_{14}\text{Cu}_{24}$ metallic glass under different pressure. The black lines in (a) and (b) show the changes of slope. The arrows in (b) show the interchange of status between peak and shoulder.

As expected, the relations of $P-r_1$ and $P-Q_1$ suggest a structural change in the short and medium range length scale, respectively, as shown in Fig. 3(a) and (b). Both Q_1 and r_1 shift with a relatively fast pace within pressure range from 10.2 to 23.8 GPa, a transition region. This structural change characterized by $P-r_1$ and $P-Q_1$ is coincident with the evolutions of both $S(Q)$ and PDFs observed in Fig. 1. Furthermore, the changes in the short and medium range orders are linked to the change in the long range order by a power law. The power law reflects the correlation between changes in the relative atomic volume and the Q_1 of structure factor $S(Q)$ as well as the nearest-neighbor distance r_1 under compressed conditions by equations [20–22]

$$\frac{V}{V_0} = \left(\frac{Q_{10}}{Q_1}\right)^{2.5} \quad \text{or} \quad \frac{V}{V_0} = \left(\frac{r_{10}}{r_1}\right)^{2.5}, \quad (2)$$

where V_0 is the average atomic volume, Q_{10} is the first peak position of structure factor $S(Q)$ and r_{10} is the nearest-neighbor distance under ambient pressure conditions. In this work, a normalized first peak position Q_1 with a power of 2.5 is used to estimate the relative volume V/V_0 change with the pressure. The relative volume V/V_0 variation as a function of pressure is shown in Fig. 3(c). The average atomic volume decreases with a fast pace at the transition region and the changes exhibit a trend similar to that of both Q_1 and r_1 as a function of pressure. Two amorphous states,

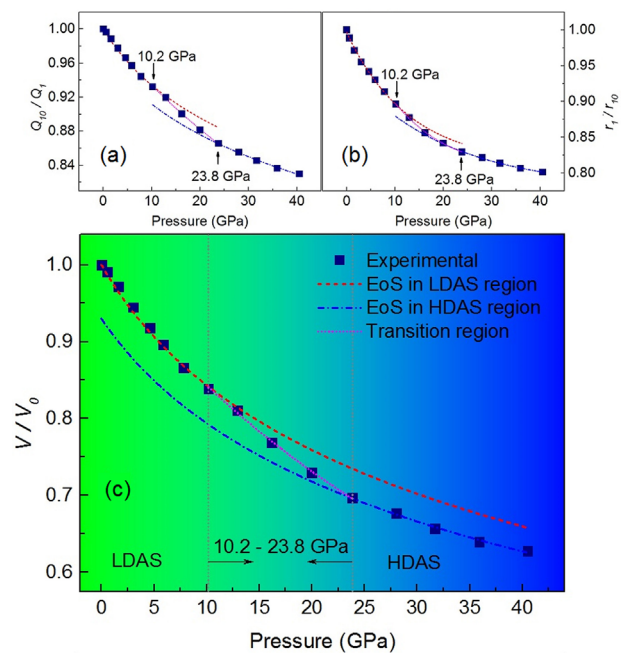


Figure 3 Pressure dependence of (a) normalized first peak position Q_1 , (b) normalized nearest-neighbor distance r_1 and (c) relative volume V/V_0 , where Q_{10} , r_{10} , and V_0 are initial first peak position, nearest-neighbor distance, and volume, respectively. In (c), the red and blue line show the EoS fitting results at LDAS region and HDAS region, respectively. The pink line is for transition region.

LDAS and HDAS, are separated by the transition region. The transformation revealed by pressure-volume relation in $\text{La}_{43.4}\text{Pr}_{18.6}\text{Al}_{14}\text{Cu}_{24}$ metallic glass exhibits an anomalous compressed region that the volume collapse takes place continuously and undergoes a broad pressure range rather than abruptly at a certain pressure point. This phenomenon is different from the typical first-order polyamorphic transition in amorphous H_2O [23], displaying a discontinuous volume change. However, such phenomenon is not uncommon in metallic glasses, such as, polyamorphic transition in $\text{Ce}_{55}\text{Al}_{45}$ metallic glass within a smooth and continuous transition region between 2 and 13.5 GPa; $\text{Ce}_{75}\text{Al}_{25}$ metallic glass within a region between 1.5 and 5 GPa [7, 8]. This continuous and broad transition range is considered as the generality for polyamorphic transition of metallic glasses. Using the second-order Birch–Murnaghan equation of state (EoS) to fit the relative volume V/V_0 under pressure, the isothermal bulk moduli are determined as $B_0 = 41.2(5)$ and $46.1(3)$ GPa at different state regions, respectively, displaying a discontinuousness of isothermal bulk modulus, as shown in Fig. 3(c). The volume difference between the LDAS and HDAS is about 7% at ambient pressure and about 14.2% within the transition region.

The change of structure under high pressure is also revealed by the ratio between the second and the first peak positions Q_2/Q_1 . The scattering intensity of glass can be expressed by Debye formula $I(q) = \sum f_i f_j \sin(qr_{ij})/qr_{ij}$, where r_{ij} is the average distance between atoms i and j , and f_i is the form factor of the i th atom. Suppose the pair atomic distance r_{ij} changes with pressure by the same factor $r_{ij}(P) = r_{ij}(1 + a \times P) = r_{ij} \times k$, the scattering intensity $I'(q/k)$ should be equal to $I(q/k)$. Thus, the ratio of the second to the first peak position Q_2/Q_1 would be a constant at various pressures in the case that the structure remains unchanged [10]. In $\text{La}_{43.4}\text{Pr}_{18.6}\text{Al}_{14}\text{Cu}_{24}$ metallic glass, the ratio of peak positions Q_2/Q_1 changes as a function of pressure, as shown in Fig. 4(a), which suggests a structure changes induced by pressure in short and medium range order scale. Furthermore, the relationship between the first peak and the splitting second peak as a function of pressure is indicative of some type of polytetrahedral short range order [13, 24]. Defining the position of the shoulder on second peak as $Q_{2\text{shoulder}}$ and using two Gaussian functions to fit the second peak, the ratios of peak positions show $Q_{2\text{shoulder}}/Q_1$ varying from 1.87 to 1.95 and Q_2/Q_1 varying

from 1.65 to 1.69 with increased pressure, as displayed in Fig. 4. Compared with a perfect icosahedron short range order, $Q_{2\text{shoulder}}/Q_1 = 2.04$ and $Q_2/Q_1 = 1.71$ [25], short range order changes in the $\text{La}_{43.4}\text{Pr}_{18.6}\text{Al}_{14}\text{Cu}_{24}$ metallic glass under pressure precede from a distortional icosahedron to a more perfect one. This means that the system becomes more ordered with increased pressure. This conclusion also can be drawn from the fact that the oscillation of the third peak around unit gradually enhances with increasing pressure in reciprocal space and that all peaks in real space become sharper as the pressure increases. According to changes of both $Q_{2\text{shoulder}}/Q_1$ and Q_2/Q_1 as a function of pressure, the polyamorphic transformation in the $\text{La}_{43.4}\text{Pr}_{18.6}\text{Al}_{14}\text{Cu}_{24}$ metallic glass under pressure is thus mainly related to the reduction of icosahedra distortion with a different pace leading to volume collapse. Whereas, this evolution of deformed icosahedra should be radically associated with electronic transformation.

Numerous crystalline polymorphic transitions in pure lanthanide elements, and lanthanide based alloys and compounds are caused by $4f$ electrons delocalization of lanthanide elements [12, 26–29]. This suggests that polymorphic transitions in these alloys and compounds inherit from those of the lanthanide elements, strongly related to the $4f$ electronic state. The inheritance was also proposed in lanthanide-based metallic glasses [14]. In the $\text{La}_{43.4}\text{Pr}_{18.6}\text{Al}_{14}\text{Cu}_{24}$ metallic glass system, although La, as a solvent element, is a member of lanthanide family, there is an absence of $4f$ electron. Previous research on La-based metallic glass suggests an absence of polyamorphic transition, despite exhibiting a local structure change in short range length scale [13]. Furthermore, the polyamorphism transformation in metallic glasses resulting from coordination increase under pressure was considered to be impossible due to their densely packed and already maximized coordination number of random nearest neighbors [8, 11]. Hence, considering Pr element with $4f^2(5d6s)^3$ electron configuration, the polyamorphic transformation in $\text{La}_{43.4}\text{Pr}_{18.6}\text{Al}_{14}\text{Cu}_{24}$ metallic glass is not attributed to La element but to Pr element although Pr component is a relatively lower quantity solute. A Pr atom in the trivalent state has a smaller atomic volume than in the divalent state. This results in a striking decrease in average bond length, which coincides with the change of icosahedral distortion and volume collapse. The transition region is generally different depending on the content of element inheriting electronic transition in metallic glass despite of the same mechanism of pressure-induced phase transformation. Such as, the transition region between 21 GPa and 37 GPa in $\text{Pr}_{75}\text{Al}_{25}$ [30] is distinctly different from that of this work; different transition regions also display in Ce-based metallic glass due to different composition of Ce; so does in Ca-based metallic glass [31]. Different pressure medium might be another possible factor for the difference of transition region between $\text{Pr}_{75}\text{Al}_{25}$ and $\text{La}_{43.4}\text{Pr}_{18.6}\text{Al}_{14}\text{Cu}_{24}$. Low Pr content in metallic glasses results in the volume collapse, 7%, smaller than those of lanthanide-solvent metallic

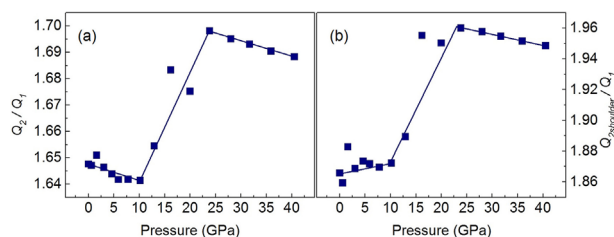


Figure 4 (a) Q_2/Q_1 and (b) $Q_{2\text{shoulder}}/Q_1$ in $\text{La}_{43.4}\text{Pr}_{18.6}\text{Al}_{14}\text{Cu}_{24}$ metallic glass as a function of pressure, respectively.

glasses, such as, volume collapses 14% in $Ce_{55}Al_{45}$ [7]. Based on previous study [14], it is proposed that polyamorphic transition in the metallic glasses containing lanthanide element, not only lanthanide-solvent but also lanthanide-solute, inherits from crystalline polymorphic transitions related to the 4f electronic state.

4 Conclusions $La_{43.4}Pr_{18.6}Al_{14}Cu_{24}$ metallic glass, a lanthanide-solute metallic glass, was studied under pressure using synchrotron X-ray total scattering method. A polyamorphic transition is observed from LDAS to HDAS, accompanying a 7% volume collapse, induced by pressure in $La_{43.4}Pr_{18.6}Al_{14}Cu_{24}$ metallic glass. The structure change is also reflected in short range and medium range length scale besides the long range length scale. This polyamorphism transformation suggests lanthanide element in metallic glass inherits from the 4f electronic state of the pure lanthanide element. The conclusion is a supplement to research on polyamorphic lanthanide-based metallic glasses.

Acknowledgements This work was performed at Argonne National Laboratory and use of the Advanced Photon Source was supported by the US Department of Energy, Office of Science, Office of Basic Energy Sciences, under contract No. DE-AC02-06CH11357. This work was supported by National Natural Science Foundation of China (U1530402, 11374075), Heilongjiang Province Science Fund for Distinguished Young Scholars (JC201005), Heilongjiang Natural Science Foundation (E200948), Longjiang Scholar, the Fundamental Research Funds for the Central Universities (HIT. BRET1.2010002, HIT. IBRSEM.A.201403), HIT-Argonne Overseas Collaborative Base Project, and Chinese Scholarship Council.

References

- [1] R. L. C. Vink and G. T. Barkema, *Phys. Rev. Lett.* **89**, 076405 (2002).
- [2] O. Mishima, L. D. Calvert, and E. Whalley, *Nature* **314**, 76 (1985).
- [3] C. Meade, R. J. Hemley, and H. K. Mao, *Phys. Rev. Lett.* **69**, 1387 (1992).
- [4] P. F. McMillan, M. Wilson, D. Daisenberger, and D. Machon, *Nature Mater.* **4**, 680 (2005).
- [5] T. Morishita, *Phys. Rev. Lett.* **93**, 055503 (2004).
- [6] A. L. Greer, *Science* **267**, 1947 (1995).
- [7] H. W. Sheng, H. Z. Liu, Y. Q. Cheng, J. Wen, P. L. Lee, W. K. Luo, S. D. Shastri, and E. Ma, *Nature Mater.* **6**, 192 (2007).
- [8] Q. S. Zeng, Y. Ding, W. L. Mao, W. Yang, S. V. Sinogeikin, J. Shu, H. K. Mao, and J. Z. Jiang, *Phys. Rev. Lett.* **104**, 105702 (2010).
- [9] Q. S. Zeng, Y. Z. Fang, H. B. Lou, Y. Gong, X. D. Wang, K. Yang, A. G. Li, S. Yan, C. Lathe, F. M. Wu, X. H. Yu, and J. Z. Jiang, *J. Phys.: Condens. Matter* **22**, 375404 (2010).
- [10] Q. Luo, G. Garbarino, B. Sun, D. Fan, Y. Zhang, Z. Wang, Y. Sun, J. Jiao, X. Li, P. Li, N. Mattern, J. Eckert, and J. Shen, *Nature Commun.* **6**, 5703 (2015).
- [11] H. W. Sheng, W. K. Luo, F. M. Alamgir, J. M. Bai, and E. Ma, *Nature* **439**, 419 (2006).
- [12] Y. C. Zhao, F. Porsch, and W. B. Holzapfel, *Phys. Rev. B* **49**, 815 (1994).
- [13] H. W. Sheng, E. Ma, H. Z. Liu, and J. Wen, *Appl. Phys. Lett.* **88**, 171906 (2006).
- [14] G. Li, Y. Y. Wang, P. K. Liaw, Y. C. Li, and R. P. Liu, *Phys. Rev. Lett.* **109**, 125501 (2012).
- [15] A. P. Hammersley, *J. Appl. Crystallogr.* **49**, 646 (2016).
- [16] K. W. Chapman, P. J. Chupas, G. J. Halder, J. A. Hriljac, C. Kurtz, B. K. Greve, C. J. Ruschmand, and A. P. Wilkinson, *J. Appl. Crystallogr.* **43**, 297 (2010).
- [17] X. J. Qiu, W. Thompson, and S. J. L. Billinge, *J. Appl. Crystallogr.* **37**, 678 (2004).
- [18] H. R. Wendt and F. F. Abraham, *Phys. Rev. Lett.* **41**, 1244 (1978).
- [19] R. S. Liu, D. W. Qi, and S. Wang, *Phys. Rev. B* **45**, 451 (1992).
- [20] Q. Zeng, Y. Kono, Y. Lin, Z. Zeng, J. Wang, S. V. Sinogeikin, C. Park, Y. Meng, W. Yang, H. K. Mao, and W. L. Mao, *Phys. Rev. Lett.* **112**, 185502 (2014).
- [21] D. Z. Chen, C. Y. Shi, Q. An, Q. Zeng, W. L. Mao, W. A. Goddard, and J. R. Greer, *Science* **349**, 1306 (2015).
- [22] Q. Zeng, Y. Lin, Y. Liu, Z. Zeng, C. Y. Shi, B. Zhang, H. Lou, S. V. Sinogeikin, Y. Kono, C. Kenney-Benson, C. Park, W. Yang, W. Wang, H. Sheng, H. K. Mao, and W. L. Mao, *Proc. Natl. Acad. Sci. USA* **113**, 1714 (2016).
- [23] O. Mishima, *J. Chem. Phys.* **100**, 5910 (1991).
- [24] G. W. Lee, A. K. Gangopadhyay, K. F. Kelton, R. W. Hyers, T. J. Rathz, J. R. Rogers, and D. S. Robinson, *Phys. Rev. Lett.* **93**, 037802 (2004).
- [25] K. F. Kelton, G. W. Lee, A. K. Gangopadhyay, R. W. Hyers, T. J. Rathz, J. R. Rogers, M. B. Robinson, and D. S. Robinson, *Phys. Rev. Lett.* **90**, 195504 (2003).
- [26] U. Benedict, *J. Alloys Compd.* **193**, 88 (1993).
- [27] Y. Y. Chen, Y. D. Yao, C. R. Wang, W. H. Li, C. L. Chang, T. K. Lee, T. M. Hong, J. C. Ho, and S. F. Pan, *Phys. Rev. Lett.* **84**, 4990 (2000).
- [28] A. Chatterjee, A. K. Singh, A. Jayaraman, and E. Bucher, *Phys. Rev. Lett.* **27**, 1571 (1971).
- [29] A. Jayaraman, A. K. Singh, A. Chatterjee, and S. U. Devi, *Phys. Rev. B* **9**, 2513 (1974).
- [30] C. L. Lin, A. S. Ahmad, H. B. Lou, X. D. Wang, Q. P. Cao, Y. C. Li, J. Liu, T. D. Hu, D. X. Zhang, and J. Z. Jiang, *J. Appl. Phys.* **114**, 213516 (2013).
- [31] H. B. Lou, Y. K. Fang, Q. S. Zeng, Y. H. Lu, X. D. Wang, Q. P. Cao, K. Yang, X. H. Yu, L. Zheng, Y. D. Zhao, W. S. Chu, T. D. Hu, Z. Y. Wu, R. Ahuja, and J. Z. Jiang, *Sci Rep.* **2**, 376 (2012).